

Charge modulation driven Fermi surface of Pb-Bi2201

L. Dudy¹, B. Müller¹, B. Ziegler¹, A. Krapf¹, H. Dwelk¹, O. Lübben¹,
R.-P. Blum¹, V. P. Martovitsky^{2*}, C. Janowitz¹, R. Manzke¹

¹Humboldt-Universität zu Berlin, Institut für Physik, Newtonstr.15, D-12489 Berlin, Germany

²Department of Low Temperature Physics, Moscow State University, Moscow 11992, Russia

(Dated: June 8, 2021)

It is well known that the (1x5) superstructure of Bi cuprate superconductors will be suppressed due to doping with Pb. Nevertheless, a Fermi surface map of $Bi_{2-y}Pb_ySr_{2-x}La_xCuO_{6+\delta}$ ($y = 0.4$ and $x = 0.4$) determined by angular resolved photoemission (ARPES) revealed additional Fermi surface features. Low energy electron diffraction and X-ray diffraction of this sample showed no sign of any superstructure. Scanning tunneling microscopy (STM), on the other hand, revealed two distinct modulations of the charge density, one of (1x32) and a second of (6x6) periodicity. The wave vectors of both modulations have been extracted and used to simulate the corresponding Fermi surface, which is compared with the experimental one. The origin of these modulations is discussed in terms of dopant ordering.

PACS numbers: 74.25.Jb, 79.60.Bm, 74.72.Hs, 68.37.Ef

Among the essential features determining the microscopic electronic properties of high temperature (HTc) superconductors the Fermi surface (FS) topology and the low energy excitations at the Fermi energy (E_F) play a key role. Over the last years important progress has been achieved by ARPES on various HTc materials from which $Bi_2Sr_2CaCu_2O_{8+\delta}$ (Bi2212) is the most commonly studied. To investigate intrinsic features it was found more appropriate to study crystals with partial substitution of Bi by Pb, i.e. Pb-Bi2212, to suppress the (1x5) superstructure in the BiO planes which could lead to unwanted diffraction replica [1] and mask other important modulations of the electron system like e.g. charge inhomogeneities/Wigner crystallization or stripes. Over the last years it became evident that phase separations due to strong correlations and structural and electronic inhomogeneities on an atomic scale are essential ingredients to HTc physics. Elastic neutron scattering experiments on $La_{1.6-x}Nd_{0.4}Sr_xCuO_4$ can be interpreted as the occurrence of charge and spin separation leading even to a static stripe-like arrangement near 1/8 doping [2]. Also scanning tunneling microscopy (STM) has revealed spatial variations of the quasiparticle density of states forming a checkerboard-like structure [3].

In this publication the ramification of structural and electronic ordering on the FS of optimally lead doped $Bi_{2-y}Pb_ySr_{2-x}La_xCuO_{6+\delta}$ (Pb-Bi2201) below the scale set up by the well known (1x5) superstructure will be discussed. The single-layer Pb-Bi2201 compound can be regarded as a prototype material to measure the almost undisturbed single CuO_2 layer, the crucial part of HTc superconductors and therefore serves as a reference material for the commonly studied double layered Bi2212. An influence from the (1x5) superstructure as well as

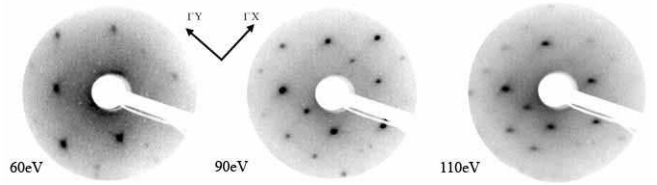


FIG. 1: LEED-patterns of optimally doped Pb-Bi2201 for different electron energies.

from bilayer splitting known for Bi2212 can be ruled out [1]. We will show by analysis of STM patterns that two main, long range modulations of one-dimensional and two-dimensional character exist. Modeling the FS with inclusion of these two modulations shows striking coincidence with the measured one by ARPES.

Single crystals of Pb-Bi2201 were grown by self flux technique. The samples were characterized by energy dispersive X-ray analysis (EDX), AC-susceptibility measurements, LEED and X-ray diffraction technique. According to EDX, the crystals studied had a Pb-content of $y = 0.41 \pm 0.06$ and a La-content of $x = 0.44 \pm 0.10$. The samples are optimally doped with hole concentration $n_h = 0.16 \pm 0.03$ holes per Cu, $T_C^{(onset)} = 30 K \pm 2 K$, and a superconducting transition width in AC-susceptibility of $\Delta T_C^{(10\%-90\%)} = 2 - 3 K$. The lattice parameters measured by X-ray diffraction are $a=5.295 \text{ \AA}$, $b=5.322 \text{ \AA}$ and $c=24.448 \text{ \AA}$. The LEED patterns of FIG.1 reveal sharp spots and no sign of a superstructure over a sufficiently large range of electron energies. In addition, the homogeneity of the samples was controlled by moving the electron beam across the sample surface.

X-ray diffraction was done at a DRONE 2.0 diffractometer with CuK_λ -radiation and a graphite monochromator. We used high resolution geometry with a narrow slit and a fixed pulse counter giving an angular resolution of 0.02° . The crystal was found to be highly perfect. The only structural defect in these crystals is a twisting along

*permanent address: Lebedev Physical Institute, Russian Academy of Science, Leninskii pr. 53, Moscow, 11991 Russia

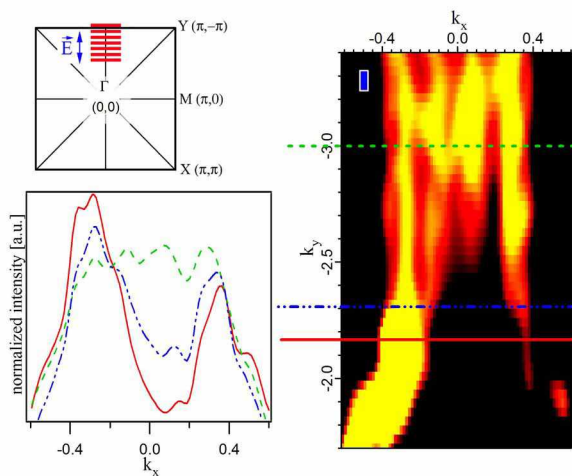


FIG. 2: **Upper left:** First Brillouin zone of a CuO_2 plane and the region of measurements. The direction of the electrical field vector applied in the ARPES experiment is indicated by an arrow. **Right:** Fermi surface map of $Bi_{2-y}Pb_ySr_{2-x}La_xCuO_{6+\delta}$ with Pb $y = 0.41$ and La $x = 0.44$. The experimental resolution is indicated by the square in the upper left corner. The density of points was doubled in each dimension by interpolation with a cubic spline. **Lower left:** Momentum distribution curves taken at E_F along three directions of the Brillouin zone as indicated by the lines in the FS map.

the c -axis. The twisting of adjacent layers in the same crystal block is of about $0.1 - 0.3^\circ$, whereas between different blocks it reaches $3 - 4^\circ$. In order to test the crystal for even weak modulations with large periodicity we used the strongest reflections, i.e. the $(0\ 0\ L)$ series. For these reflections we measured the rocking curves along the $[2\ 0\ 0]$ and $[0\ 2\ 0]$ directions. In presence of a modulation one would expect a shift of the corresponding rocking curve maxima for different L reflections. For example, a modulation with 32 periods would have an angle of 0.51° between $(0\ 0\ 16\ 0)$ and $(0\ 0\ 16\ 1)$ and an angle of 1.01° between $(0\ 0\ 8\ 0)$ and $(0\ 0\ 8\ 1)$. Since these superspots have not been found it can be concluded that the crystal is free of structural modulations.

The ARPES measurements were carried out with a Scienta SES-100 analyzer at the U125-2/10m-NIM at BESSY. All data were taken with 22 eV photon energy and a sample temperature of 25 K. The energy resolution was 18 meV. The angular resolution was 0.2 degree. E_F was determined from the Fermi-edge of an evaporated Au film. The measured region in the first Brillouin zone is shown in FIG.2. The electrical field vector was orientated parallel to the line ΓM as indicated. The components of the wave vectors are given in units in which i.e. $(k_x, k_y) = (\pi, \pi)$ denotes the X-point. We determined a FS map by integrating the spectra in an energy window of ± 10 meV around E_F . The resulting map is shown on the right side of FIG.2. One should note (i) the complex pattern far from what one would expect for

a single FS and (ii) the distinct anisotropy in the intensity with respect to the symmetry direction ΓM . This is even more obvious in the momentum distribution curves (MDC) of FIG.2. The MDC near M are more symmetric than towards Γ .

In order to find an explanation for the complicated FS and asymmetries observed by ARPES we analyzed in detail the corrugation of the charge distribution at the surface. This is determined by highly resolved STM. All measurements were performed at room temperature with $U=0.5$ V and $I=0.4$ nA. Because of the extremely low corrugation the noise level had to be better than 0.05 nm. A picture obtained at these conditions is depicted in FIG.3 (a). Due to the extreme two-dimensionality of the electronic structure of Bi2201 it was found difficult to image individual atoms. At first view only domains with an average spacing of $170\ \text{\AA}$ are visible along the b -direction. The electron density inside the almost smooth $170\ \text{\AA}$ -domains is also modulated, but at extremely low corrugation. The detailed analysis described in the following will reveal that these modulations are ordered by a (6×6) symmetry.

To obtain quantitative information on the modulations seen in STM and their effect on the Fermi surface measured by ARPES, we first determine the structure-factor $F(\vec{q})$ from the STM pattern and use this knowledge to simulate the FS. The result will be compared with the experiment.

Persistent ignoring an influence of the tip, the STM signal is proportional to the charge density $\rho(\vec{r})$. It is therefore generally possible to determine the structure-factor $F(\vec{q})$ from $\rho(\vec{r})$ directly. Similar to kinetic LEED theory the structure-factor $F(\vec{q})$ is given by the Fourier-transformed charge density $\rho(\vec{r})$:

$$F(\vec{q}) = \int d^2r e^{i\vec{q}\vec{r}} \rho(\vec{r}). \quad (1)$$

But in order to reduce the noise level of the STM data it is more adequate to apply the autocorrelation function of the charge density defined as

$$\rho_- \circ \rho(\vec{u}) = \frac{1}{V} \int d^2r \rho(\vec{r}) \rho(\vec{r} + \vec{u}). \quad (2)$$

With the normalization $\tilde{\rho}(\vec{r}) = \rho(\vec{r}) - \frac{1}{V} \int_V d\vec{r}' \rho(\vec{r}')$ the autocorrelation acts as a good natural noise-filter. The autocorrelation $\rho_- \circ \rho(\vec{u})$ of the STM data of a $30\text{nm} \times 30\text{nm}$ region is shown in FIG. 3(b). The square of the structure-factor can now be computed by use of the Wiener-Khinchin theorem [4] as the absolute value of the Fourier-transformed autocorrelation function, i.e.

$$F(\vec{q})^2 = \left| \int d^2u e^{i\vec{q}\vec{u}} \tilde{\rho}_- \circ \tilde{\rho}(\vec{u}) \right| \quad (3)$$

which is shown in FIG. 3(c). Due to the normalization and the finite dimension of the STM pattern we lose the information of zero wavelength and obtain therefore no peak corresponding to the nearly undisturbed $\rho(\vec{r})$,

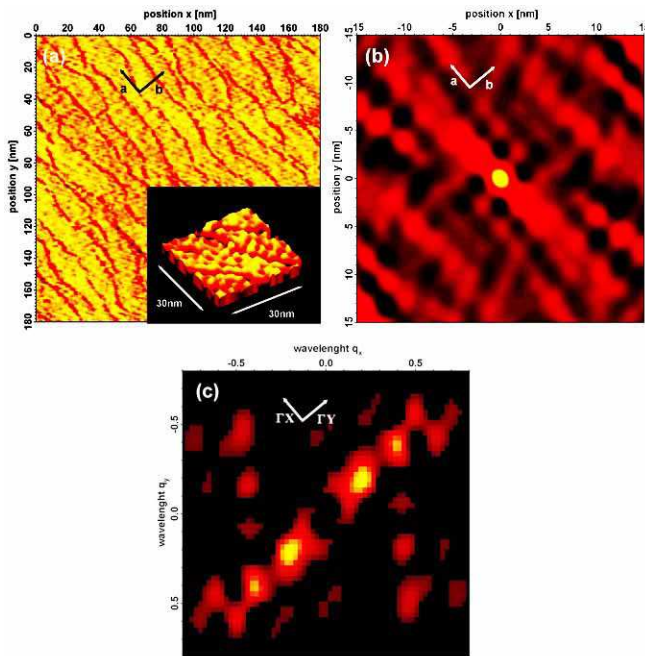


FIG. 3: (a) Topological STM signal of $Bi_{2-y}Pb_ySr_{2-x}La_xCuO_{6+\delta}$ with Pb $y = 0.42$ and La $x = 0.40$. All measurements were done at room temperature with $U = 0.5$ V and $I = 0.4$ nA. In the inset an area of 30 nm \times 30 nm is magnified. (b) The autocorrelation $\rho_- \circ \rho(\vec{u})$ derived for the topological STM signal shown in the inset of (a). (c) The squared structure-factor $F(\vec{r})^2$ as calculated by Eq. (3) from the autocorrelation function shown in (b). The density of data points was doubled in both dimensions by interpolation with a cubic spline.

TABLE I: Position, intensity, and periodicity the peaks found in the Fourier-transformed autocorrelation function $F(\vec{q})^2$ depicted in FIG. 3(c). Here the positions are given in fractions of π , i.e. $(q_x, q_y) = (1, 0)$ means the M-point.

$\pm q_x$	$\pm q_y$	rel. int.	periodicity	comment
0	0	1	undisturbed	+ 1st.order (1x32)
0,06	-0,06	0,42	16.5 b	2nd. order (1x32)
0,12	-0,12	0,21	8 b	3rd. order (1x32)
0,14	0,15	0,08	6.5 a	(6x6)
0,16	-0,16	0,07	6 b	

representing the main FS and the first order of a (1x32) modulation. On the other hand, a number of additional peaks are detectable in $F(\vec{q})^2$ which are listed in TAB. I. With highest intensity one identifies the second order of a (1x32) modulation due to the one-dimensional ordering of the 170 Å-domains. Even the third order of this modulation is quite intense. The ordering within the flat regions of the 170 Å-domains yields a two-dimensional (6x6) symmetry. The weak intensity of about 8% is in line with the extremely low corrugation observed by STM.

Taking into account the periodic charge modulations

found by STM the signal of the photoelectrons near E_F is given by

$$I(\vec{k}, \omega = 0, T) \simeq \int d^2q I_0(\vec{k} + \vec{q}, \omega = 0, T) F(\vec{q})^2. \quad (4)$$

For I_0 , the bare FS without modulations, the intensity of the photoemission signal is the Fermi function $f(\omega, T)$ times the spectral function $A(\vec{k}, \omega, T)$ (the transition matrix element was set constant):

$$I_0(\vec{k}, \omega, T) \simeq f(\omega, T) A(\vec{k}, \omega, T). \quad (5)$$

We used a simplified form of the empirical spectral function $A(\vec{k}, \omega, T)$ of Kordyuk et al. [5]:

$$A(\vec{k}, \omega, T) \simeq \frac{\Sigma''}{(\omega - E(\vec{k}))^2 + \Sigma''^2}. \quad (6)$$

The imaginary part of the self energy is given as $\Sigma'' = \sqrt{(\alpha\omega)^2 + (\beta T)^2}$. The energy and temperature dependence is controlled by the constants α and β , which were set to $\alpha = 1$ and $\beta = 1$ meV/K. For the dispersion relation $E(\vec{k})$ we took a temperature independent tight binding-like ansatz [5]

$$E(\vec{k}) = \Delta E - 2t(\cos k_x + \cos k_y) + 4t'(\cos k_x \cos k_y) - 2t''(\cos 2k_x + \cos 2k_y) \quad (7)$$

The values $\Delta E = 0.18$ eV, $t = 0.17$ eV, $t' = 0.015$ eV and $t'' = 0.039$ eV were obtained from a fit of the dispersion curves measured by ARPES at various Brillouin zone locations. With these values the normalized FS-volume gives a hole concentration of $n_h = 0.5 - V_{FS} = 0.157 \pm 0.020$ holes per Cu which is in good agreement with the experimental value of the studied Pb-Bi2201 crystal of 0.16 ± 0.03 holes per Cu.

By means of Eq. (5) to (7) one is now able to compute the Fermi surface where $F(\vec{q})$ includes the (1x32) and (6x6) modulations found by STM. The intensity of the main FS slightly broadened by the first order (1x32) was set to I_0 and adjusted to the experimental intensity. This simulated FS is shown in FIG. 4(a). Due to the two modulations additional FS features appear besides the main FS causing especially around the M ($\pi, 0$) points strong additional intensity in the simulated FS (FIG. 4(b)) in accordance with the experiment (FIG. 4(c)). Because of its two-dimensionality, the (6x6) modulation leaves the FS symmetric with respect to the Brillouin zone. The appearance of different FS intensities with respect to the quadrants is predominantly due to the one-dimensional (1x32) modulation. Such an asymmetrical intensity distribution has also been observed in other experiments using Pb-Bi2201 [6] and therefore the (1x32) modulation gives an explanation for this behavior.

Regarding the origin of these modulations, the following picture emerges: While LEED and X-ray diffraction detect a perfect lattice, STM and ARPES reveal periodic modulations. The modulations do not reveal a distinct

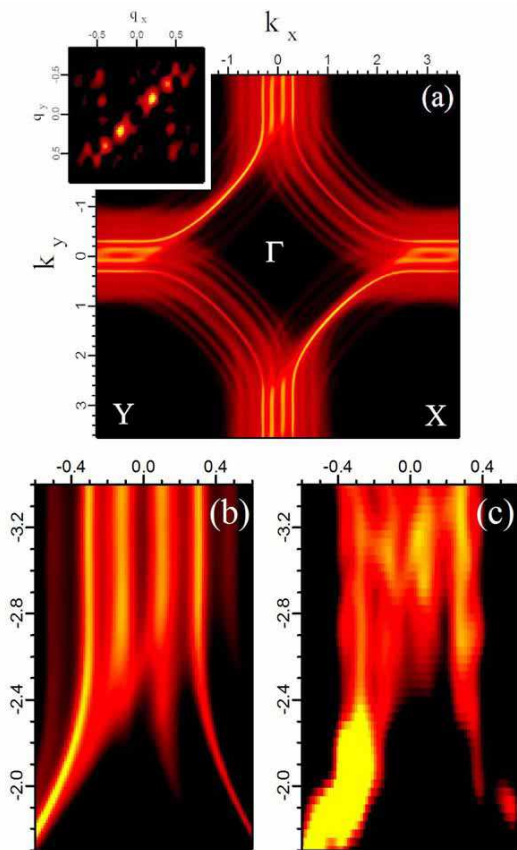


FIG. 4: (a) Simulated FS of Pb-Bi2201 using all wave vectors found in the structure-factor $F(\vec{q})^2$ by STM (see inset). (b)(c) Comparison of simulated FS (b) and measured FS (c) near M.

temperature dependence. In order to explain these observations one should mention that LEED is not sensitive

to periodic arrangements larger than the coherence zone of about 100 Å. In our case the (1x32) modulation by the 1x170 Å domains is beyond that dimension and therefore not detectable by LEED. Also modulations of low corrugation, as in our case the (6x6) structure, are hardly detectable by LEED. Also by X-ray diffraction not all possible periodic arrangements can be detected, namely: (i) periodic arrangements of the Pb and Bi atoms in the otherwise perfect lattice, and (ii) ordering of oxygen. Point (i) is due to the nearly equivalent atomic form factors of Pb and Bi, and (ii) due to the small atomic form factor of O. It could therefore be speculated that a lattice solid consisting of ordered Pb, Bi and/or O could be formed. Calculation of the thermal stability of a lattice solid in a Pb-Bi2201 structure may be done similar as e.g. [7]. It may be worth noting that oxygen ordering within the CuO-chains of $YBa_2Cu_3O_x$ is quite common [8]. It could also be speculated that the (6x6) modulation found here exhibits a familiarity to the nondispersive nanoscale modulations seen in Bi2212 [3]. For the superconducting properties it was recently discussed that modulations found at room temperature are precursors to promote an ordering of holes within the CuO_2 plane [9] or modulate the superconducting pairing interaction [10].

In summary, we have proven that a periodic modulation of the charge density exists and has profound influence on the Fermi surface and generally on the electronic structure of Pb-Bi2201 observed by ARPES.

We would like to thank the staff of BESSY and in particular G. Reichardt for excellent support during the ARPES measurements. We thank S. Rogaschewski for EDX and R. Müller for discussions. This work has been supported by the DFG, project MA2371/3. We gratefully thank Y.G. Ponomarev and the DAAD, program 'Ostpartnerschaften'.

[1] A. Damascelli et al., Rev. Mod. Phys. 75, 473 (2003) and reference therein; M.R. Norman and C. Pepin, Rep. Prog. Phys. 66, 1547 (2003) and reference therein
 [2] J. M. Tranquada et al., Nature 375, 561 (1995)
 [3] Ø. Fischer et al., Rev. Mod. Phys. 79, 353 (2007) and reference therein
 [4] N. Wiener, The Fourier Integral and Certain of its Applications, Dover Publications, New York (1958)

[5] A.A. Kordyuk et al., Phys. Rev. B 67, 64504 (2003)
 [6] T. Kondo et al., arXiv:cond-mat/0611517
 [7] K. Hoang et al., Phys. Rev. B 72, 064102 (2005)
 [8] K. Widder et al., Physica C 232, 1-2, 82 (1994)
 [9] S. Zhou et al., Phys. Rev. Lett. 98, 76401 (2007)
 [10] B.M. Andersen et al., arXiv:0704.3673 (2007)